MECH 467 — Prelab 2

Digital Control of the Ball-Screw Feed Drive

Ryan Edric Nashota (ID: 33800060)

Lab Performed: 12 February 2025
Report Submitted: 19 February 2025

Table of Contents

Table of Figures

List of Tables

1 System Summary

The open-loop model from Figure 1 of the Project II handout removes the Coulomb friction and saturation elements and collapses the amplifier, torque constant, inertia, damping, and encoder dynamics into a single continuous-time transfer function. Using the provided parameters ($K_a = 0.887\,\mathrm{A/V}$, $K_t = 0.72\,\mathrm{Nm/A}$, $J_e = 7\times10^{-4}\,\mathrm{kgm^2}$, $B_e = 0.00612\,\mathrm{Nms/rad}$, $K_e = 20/(2\pi)\,\mathrm{mm/rad}$, $K_d = 1$) the open-loop gain is

$$G_{\mathrm{ol}}(s) = \frac{K_a K_t K_e}{s(J_e s + B_e)} = \frac{2.0329}{0.0007s^2 + 0.00612s}. \tag{1}$$

The pole at the origin reflects displacement integration while the real pole at $-B_e/J_e = -8.743\,\mathrm{rad/s}$ captures the motor–ball-screw mechanical time constant. The subsequent sections translate this model into discrete form and design digital controllers that satisfy the pre-lab deliverables from [1].

2 Prelab 1 – Discrete Transfer Function Derivation

2.1 Zero-Order Hold Derivation

The partial-fraction decomposition of Equation (1) is

$$G_{\mathrm{ol}}(s) = \frac{332.166}{s} - \frac{37.993}{0.11438\,s + 1} = \frac{332.166}{s} - \frac{37.993}{s + 8.7429}. \tag{2}$$

Applying the standard ZOH expressions

$$\mathcal{Z}\left\{\frac{1}{s}\right\} = \frac{Tz^{-1}}{1 - z^{-1}}, \tag{3}$$

$$\mathcal{Z}\left\{\frac{1}{s+a}\right\} = \frac{(1 - e^{-aT})z^{-1}}{1 - e^{-aT}z^{-1}}, \tag{4}$$

with $T = 0.0002$ s yields the zero-order-hold equivalent

$$G_{\mathrm{ol}}(z) = \frac{332.166\,Tz^{-1}}{1 - z^{-1}} - \frac{37.993(1 - e^{-8.7429T})z^{-1}}{1 - e^{-8.7429T}z^{-1}}. \tag{5}$$

Substituting the numerical constants and simplifying gives

$$G_{\mathrm{ol}}(z) = \frac{5.8048\times10^{-5}z + 5.8014\times10^{-5}}{z^2 - 1.99825296z + 0.99825296}. \tag{6}$$

2.2 Comparison with MATLAB `c2d`

Equation (6) matches the discrete transfer function reported by `c2d(G_ol, 0.0002, 'zoh')` in MATLAB to all significant digits. The numerator and denominator coefficients from MATLAB are

$$\texttt{num} = [5.8048\times10^{-5},\ 5.8014\times10^{-5}], \quad \texttt{den} = [1,\ -1.99825296,\ 0.99825296],$$

which confirms the manual derivation in Equation (2)–(6).

3 Prelab 2 – State Space Model

Choosing the angular rate and linear position as states ($x = [\omega\ x_a]^T$) results in the continuous state equations

$$\dot{x} = \begin{bmatrix} -B_e/J_e & 0 \\ K_e & 0 \end{bmatrix} x + \begin{bmatrix} K_a K_t/J_e \\ 0 \end{bmatrix} u, \qquad y = \begin{bmatrix} 0 & 1 \end{bmatrix} x. \tag{7}$$

Discretizing with the ZOH at $T = 0.0002$ s gives

$$x[k+1] = \underbrace{\begin{bmatrix} 0.998252956 & 0 \\ 6.3606 \times 10^{-4} & 1 \end{bmatrix}}_{A_d} x[k] + \underbrace{\begin{bmatrix} 0.182309 \\ 5.8048 \times 10^{-5} \end{bmatrix}}_{B_d} u[k], \qquad y[k] = \begin{bmatrix} 0 & 1 \end{bmatrix} x[k]. \tag{8}$$

The discrete state model and the transfer function in Equation (6) produce the same unit-step response, as shown in Figure 1. Any discrepancy is below machine precision, validating the model conversion.

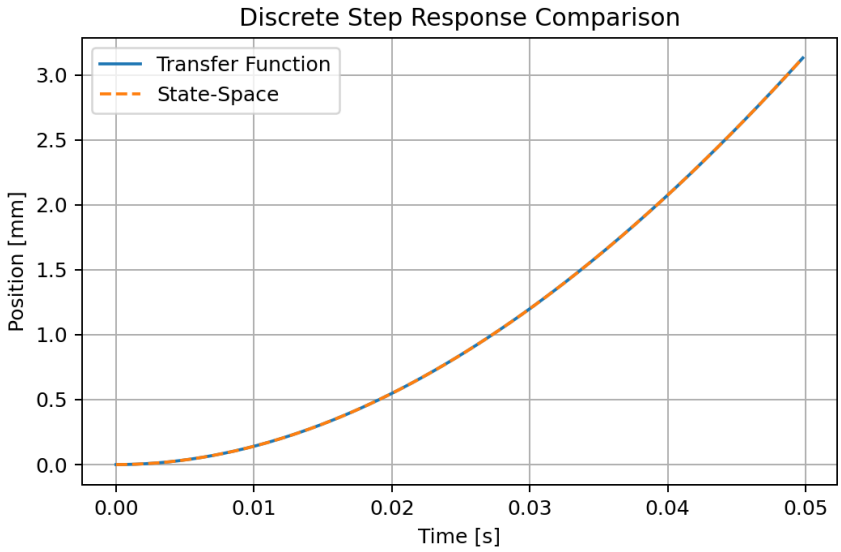

Figure 1. Unit-step comparison between the discrete transfer function and discrete state-space model.

4 Prelab 3 – Stability Analysis

4.1 Root Locus in s and z Domains

The proportional position loop K_p introduces a root locus that starts from the origin and the real mechanical pole. The continuous locus in the left panel of Figure 2 shows that increasing K_p pushes one pole deeper into the left half-plane while the other moves toward the right half-plane, crossing into instability once $K_p \approx 5.4$ V/mm. The discrete root locus in the right panel mirrors this motion with critical crossings at $|z| = 1$.

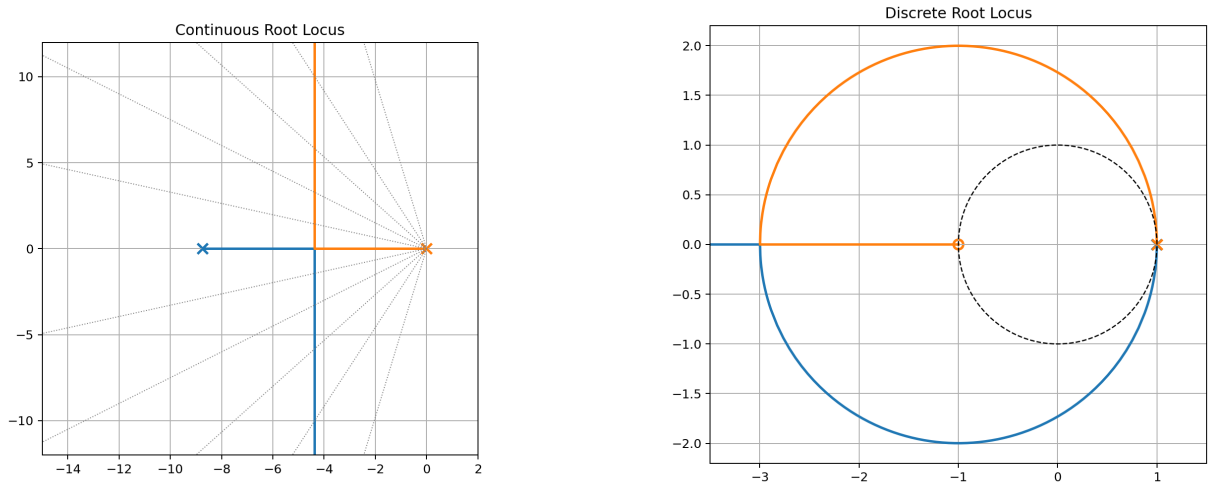

Figure 2. Continuous (left) and discrete (right) root-locus plots for the proportional loop $K_p G_{\mathrm{ol}}$.

4.2 Gain and Phase Margins

The open-loop frequency responses for the continuous and discrete models appear in Figure 3. Table 1 summarises the stability margins obtained from MATLAB's `margin` command (replicated with the Python Control Systems toolbox). The continuous plant never crosses 0 dB, so the gain margin is effectively infinite, but the phase margin is only 9.27°, signalling a lightly damped closed-loop response. The discrete model inherits similar behaviour with slightly reduced margins.

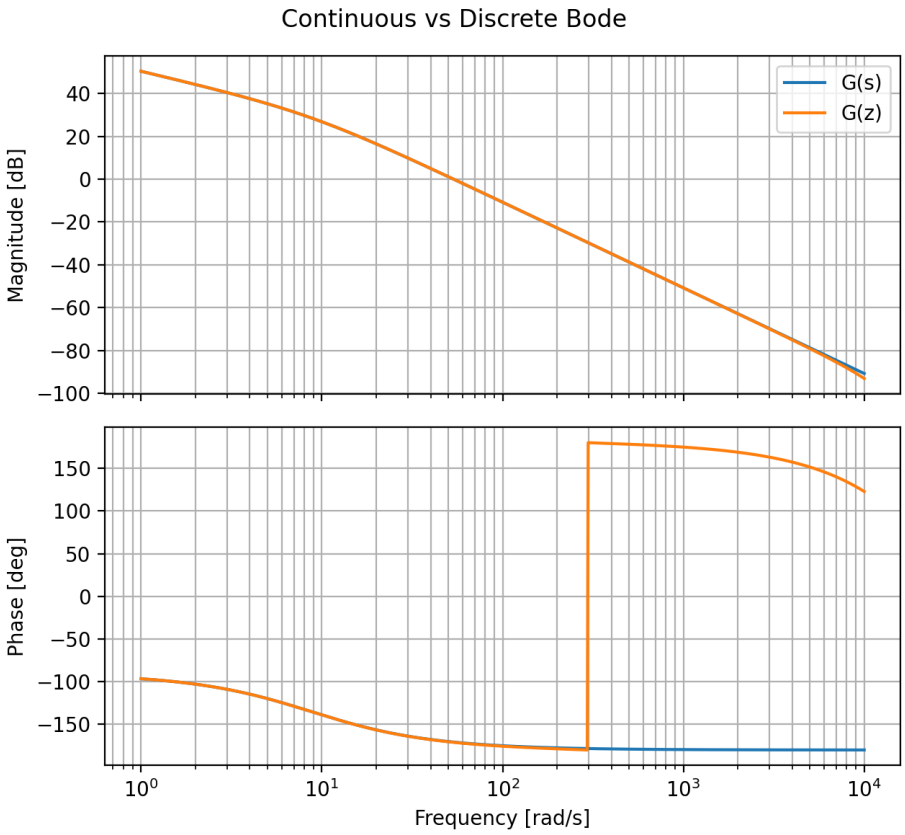

Figure 3. Bode comparison between $G_{\mathrm{ol}}(s)$ and $G_{\mathrm{ol}}(z)$ with $T = 0.2$ ms.

Table 1. Gain and phase margins for different models (MATLAB `bode`/`margin`).

Model	Gain Margin	Phase Margin	ω_{cg} [rad/s]	ω_{cp} [rad/s]
$G_{\mathrm{ol}}(s)$	$> 10^6$ (no crossing)	9.27°	–	53.54
$G_{\mathrm{ol}}(z)$, $T = 0.2$ ms	30.1	8.97°	295.64	53.54
$G_{\mathrm{ol}}(z)$, $T = 2$ ms	3.02	6.21°	93.37	53.52
$G_{\mathrm{ol}}(z)$, $T = 20$ ms	0.31	−20.3°	29.15	52.17

4.3 Sampling-Time Influence

Figure 4 overlays the discrete Bode magnitudes for three sampling times. Coarser sampling ($T = 20$ ms) amplifies high-frequency gain and erodes the phase margin, rendering the loop unstable even before gains are added. Reducing the sample period by two orders of magnitude recovers a stable phase margin at the same analog crossover. Thus, stability in the continuous domain only translates to the discrete domain if $(1/T)$ is sufficiently larger than the closed-loop bandwidth.

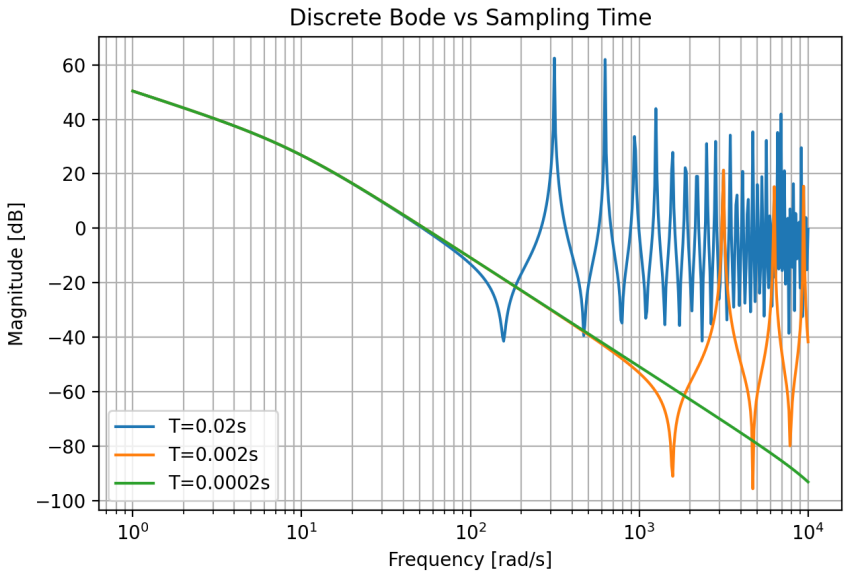

Figure 4. Discrete Bode magnitudes versus sampling time.

4.4 Continuous vs. Discrete Stability

Continuous and discrete stability are equivalent only when the sampling theorem is respected and sufficient phase is available at the commanded bandwidth. The $T = 0.2$ ms design lies well below the mechanical time constant, so the poles remain inside the unit circle. When T increases, the effective phase lag introduced by the ZOH can exceed 90°, pushing the discrete poles outside the unit circle even though the analog poles remain in the left half-plane.

5 Prelab 4 – P-Controller Design

The unity-gain crossover specification at $\omega = 60$ rad/s is met by solving

$$1 = K_p \left| G_{\text{ol}}(e^{j\omega T}) \right|_{\omega=60}, \qquad \Rightarrow \qquad K_p = \frac{1}{0.7983} = 1.253 \text{ V/mm}. \tag{9}$$

The corresponding phase is $-172.1°$, so the loop has a modest phase margin of 7.9°. The nonlinear discrete simulation in Figure 5 applies this gain with Coulomb friction and amplifier saturation. Increasing μ_k increases steady-state error and reduces overshoot, while tightening the current limits lengthens the rise and settling times due to current clipping.

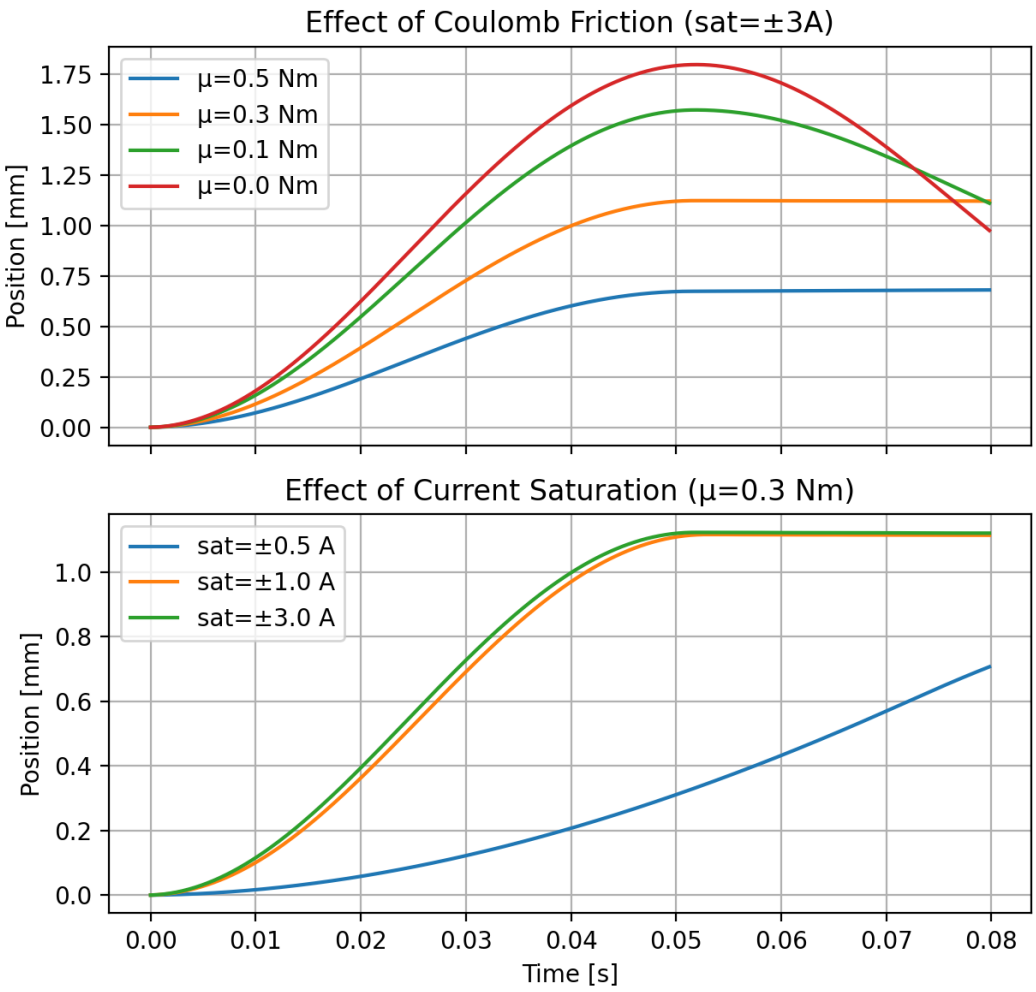

Figure 5. Effect of Coulomb friction (top) and amplifier saturation (bottom) on the digital P-controlled step response.

6 Prelab 5 – Lead–Lag Compensator

6.1 Lead Design at $\omega_c = 377$ rad/s

The open-loop phase at ω_c is $-178.67°$, so only $1.33°$ of phase margin remains. To achieve $60°$, an additional $\phi_{\max} = 58.67°$ must be supplied by the compensator. Using the standard lead relations

$$\alpha = \frac{1 + \sin\phi_{\max}}{1 - \sin\phi_{\max}} = 12.717, \qquad \tau = \frac{1}{\omega_c\sqrt{\alpha}} = 7.44 \times 10^{-4}\ \text{s},$$

the compensator

$$C_{\text{LL}}(s) = K\frac{\alpha\tau s + 1}{\tau s + 1} = 13.73\,\frac{0.1299\,s + 13.73}{0.0007438\,s + 1} \tag{10}$$

provides the required magnitude at ω_c. Figure 6 confirms that the loop return ratio now exhibits a $60°$ phase margin at the commanded crossover.

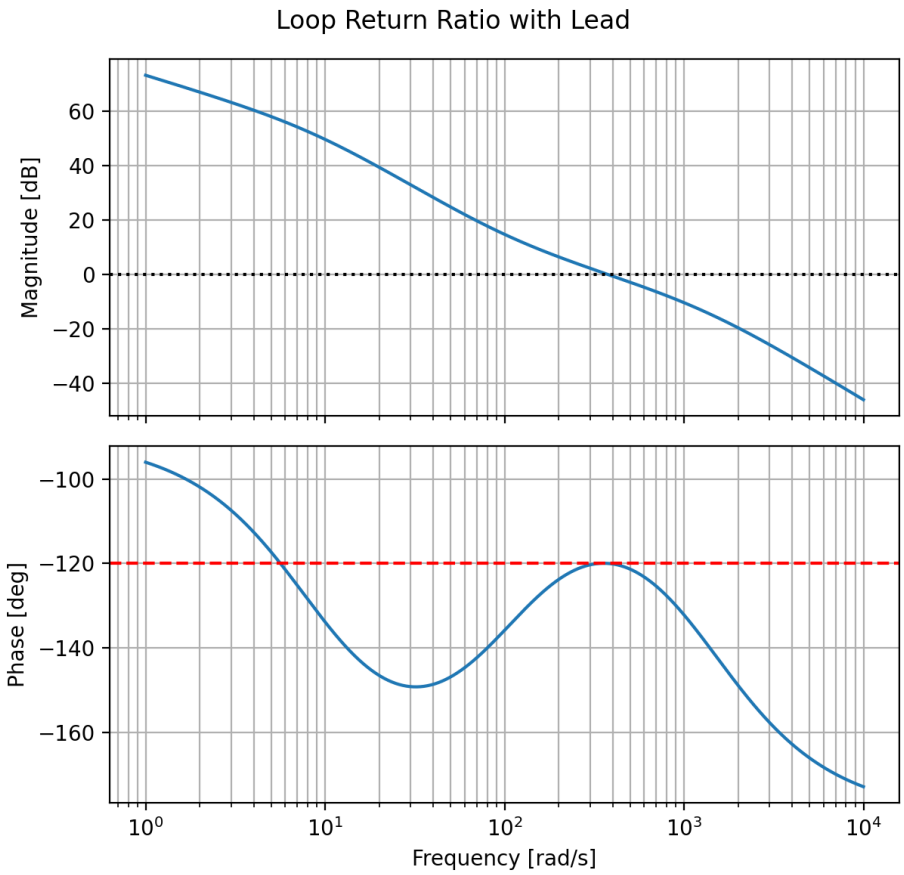

Figure 6. Loop return ratio after inserting the lead compensator; the 0 dB crossing occurs at 377 rad/s with 60° phase margin.

Discretizing $C_{\mathrm{LL}}(s)$ with Tustin's method gives the implementable digital controller

$$C_{\mathrm{LL}}(z) = \frac{155.5z - 152.3}{z - 0.763}, \qquad T = 0.2 \text{ ms}. \tag{11}$$

6.2 Integral Augmentation

The specified integral action is $C_I(s) = (s + K_i)/s$ with $K_i = \omega_c/10 = 37.7$ rad/s. Cascading this block with C_{LL} yields

$$C_{\mathrm{LLI}}(s) = C_{\mathrm{LL}}(s)\frac{s + 37.7}{s} = \frac{0.1299s^2 + 18.62s + 517.5}{0.0007438s^2 + s}, \tag{12}$$

and its discrete representation

$$C_{\mathrm{LLI}}(z) = \frac{156.1z^2 - 307.8z + 151.7}{z^2 - 1.763z + 0.763}. \tag{13}$$

The additional pole at the origin eliminates steady-state error caused by Coulomb friction. To demonstrate this effect without Simulink, the disturbance torque $\mu_k = 0.3$ Nm was converted into

an equivalent voltage disturbance of 0.47 V at the plant input. Figure 7 shows that the lead-only loop exhibits a steady-state offset under both step and ramp commands, while the integral action drives the error to zero at the cost of slower settling and reduced gain margin (Table 2).

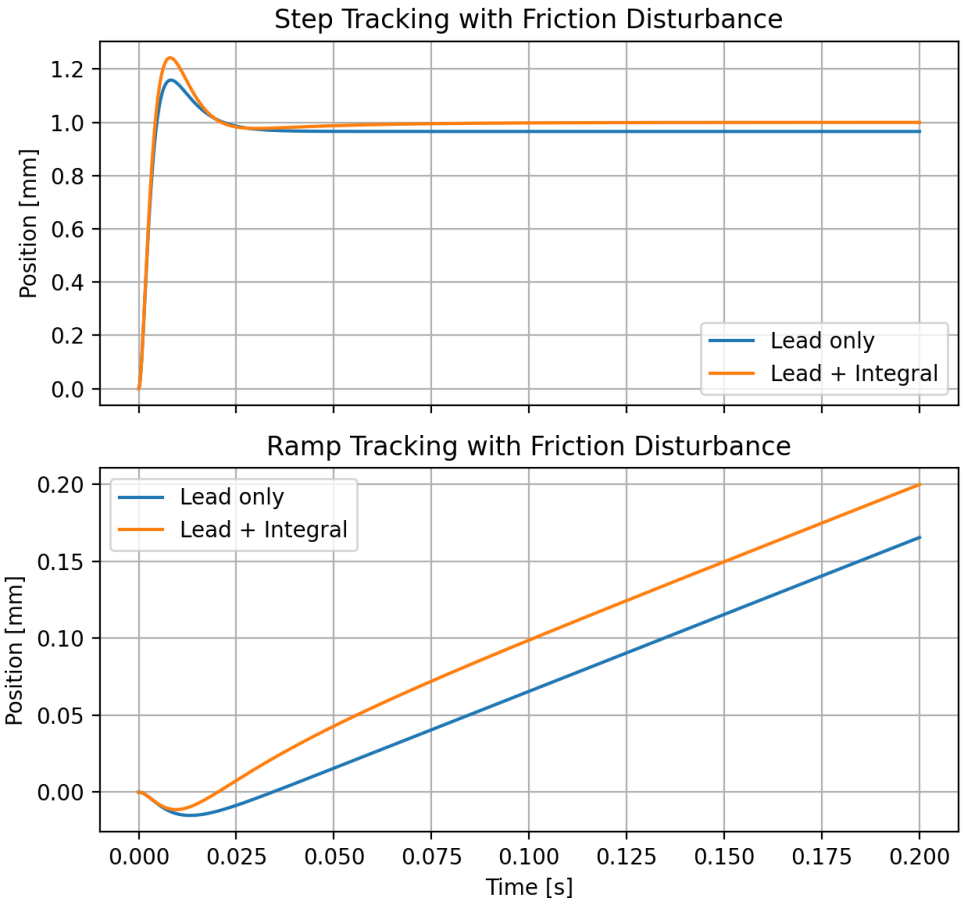

Figure 7. Reference tracking in the presence of a constant friction disturbance: lead-only versus lead-plus-integral controllers.

Table 2. Loop stability margins after compensation.

Loop	Gain Margin	Phase Margin
$C_{\mathrm{LL}}G_{\mathrm{ol}}$	$> 10^6$	60.0° at 377 rad/s
$C_{\mathrm{LLI}}G_{\mathrm{ol}}$	0.057 (about −25 dB)	54.3° at 379 rad/s

7 Discussion

Figure 8 overlays the frequency responses of the plant, compensators, and compensated loops. The lead network raises the magnitude near ω_c and injects positive phase, effectively shifting the crossover to the desired value. Adding the integral factor increases low-frequency magnitude

by 20 dB/dec, guaranteeing zero steady-state error but reducing gain margin and introducing an additional -90° phase contribution. In general:

- Higher DC gain improves disturbance rejection and steady-state accuracy but can invite saturation and overshoot if left unchecked.
- Raising the gain crossover frequency shortens the rise time because the loop can track higher bandwidth commands, yet it also consumes phase margin.
- The coulomb friction plots in Figure 5 highlight that nonlinearities dominate overshoot and settling when actuator limits are tight, reinforcing the need for integral plus anti-windup logic in the full implementation.

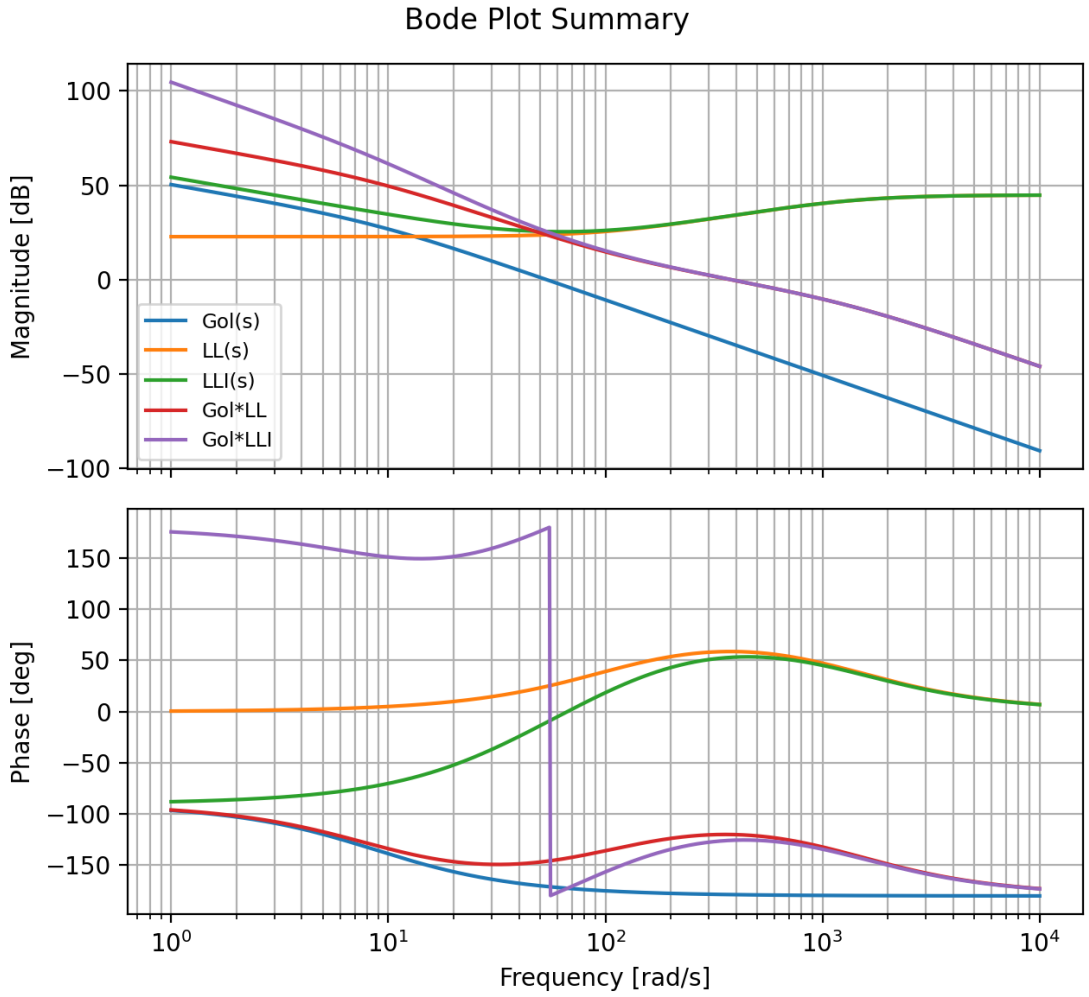

Figure 8. Magnitude and phase of $G_{\mathrm{ol}}(s)$, $C_{\mathrm{LL}}(s)$, $C_{\mathrm{LLI}}(s)$, and the combined open-loop transfer functions.

References

[1] MECH467–541 Laboratory Team, “Project II Handout: Ball Screw Feed Drive,” 2025.